Journal of Biomechanics 42 (2009) 1384–1389

Contents lists available at ScienceDirect

Journal of Biomechanics

journal homepage: www.elsevier.com/locate/jbiomech
www.JBiomech.com

2008 ASB Young Scientist Post-Doctoral Award

Passive mechanical properties of the lumbar multifidus muscle support its role as a stabilizer ☆

Samuel R. Ward [a,b,c], Akihito Tomiya [a], Gilad J. Regev [a], Bryan E. Thacker [c], Robert C. Benzl [a], Choll W. Kim [a], Richard L. Lieber [a,c,*]

[a] Department of Orthopaedic Surgery, University of California and Veterans Administration Medical Centers, San Diego, USA
[b] Department of Radiology, University of California and Veterans Administration Medical Centers, San Diego, USA
[c] Department of Bioengineering, University of California and Veterans Administration Medical Centers, San Diego, USA

ARTICLE INFO

Article history:
Accepted 25 September 2008

Keywords:
Lumbar multifidus
Muscle mechanics
Lumbar spine

ABSTRACT

The purpose of this study was to compare the passive mechanical properties and titin isoform sizes of the multifidus, longissimus, and iliocostalis muscles. Given our knowledge of each muscle's architecture and the multifidus' operating range, we hypothesized that multifidus would have higher elastic modulus with corresponding smaller titin isoforms compared to longissimus or iliocostalis muscles. Single-fiber and fiber-bundle material properties were derived from passive stress–strain tests of excised biopsies ($n = 47$). Titin isoform sizes were quantified via sodium dodecyl sulfate-vertical agarose gel electrophoresis (SDS-VAGE) analysis. We found that, at the single-fiber level, all muscles had similar material properties and titin isoform sizes. At the fiber-bundle level, however, we observed significantly increased stiffness (~45%) in multifidus compared to longissimus and iliocostalis muscles. These data demonstrate that each muscle may have a different scaling relationship between single-fiber and fiber-bundle levels, suggesting that the structures responsible for higher order passive mechanical properties may be muscle specific. Our results suggest that divergent passive material properties are observed at size scales larger than the single cell level, highlighting the importance of the extracellular matrix in these muscles. In addition to architectural data previously reported, these data further support the unique stabilizing function of the multifidus muscle. These data will provide key input variables for biomechanical modeling of normal and pathologic lumbar spine function and direct future work in biomechanical testing in these important muscles.

Published by Elsevier Ltd.

1. Introduction

The posterior paraspinal muscles provide dynamic stability to the spinal column (Bogduk et al., 1992). Numerous studies have described the anatomical (Macintosh and Bogduk, 1986; Macintosh et al., 1993; Stokes and Gardner-Morse, 1999; Delp et al., 2001; Rosatelli et al., 2008) and histochemical (Rantanen et al., 1994) properties of these muscles with the goal of understanding normal and pathological spinal function. Similarly, imaging studies of the multifidus and other muscles have revealed pathologic changes associated with other spinal abnormalities such as chronic low back pain (Flicker et al., 1993; Parkkola et al., 1993), disk herniation (Zhao et al., 2000), scoliosis (Chan et al., 1999), and degenerative lumbar kyphosis (Kang et al., 2007). Paradoxically, surgery designed to treat these spinal disorders actually disrupt these muscles, and in turn, may lead to significant secondary structural and functional deficits (Skaf et al., 2005; Hazard, 2006; Sasaoka et al., 2006; Gille et al., 2007) which has been correlated with the development of post-surgical failed-back syndrome (Sihvonen et al., 1993; Turner et al., 2004; Taylor, 2006; Boswell et al., 2007).

The structure, function, and design of skeletal muscle has primarily been studied in the upper (Jacobson et al., 1992; Lieber et al., 1992) and lower extremities (Wickiewicz et al., 1983; Friederich and Brand, 1990), with very little data available for axial musculature. One universal finding in studies of extremity muscle is that skeletal muscle architecture, defined as the number and orientation of muscle fibers within a muscle, is the only accurate predictor of function (Powell et al., 1984; Lieber and Friden, 2001). Architectural properties of many spinal muscles were reported by Delp et al. (2001). However, it has been recently demonstrated that the multifidus muscle has a unique design amongst the

☆ IRB: Each author certifies that his or her institution has approved the protocol for this investigation and that all investigations were conducted in conformity with ethical principles of research.

* Corresponding author at: Department of Orthopaedic Surgery (9151), UC San Diego and VA Medical Center, 3350 La Jolla Village Drive, San Diego, CA 92161. Tel.: +858 552 8585x7016; fax: +858 552 4381.
E-mail address: rlieber@ucsd.edu (R.L. Lieber).

0021-9290/$ - see front matter Published by Elsevier Ltd.
doi:10.1016/j.jbiomech.2008.09.042

posterior spinal muscles; to stabilize the lumbar spine based on its very short fiber length, large physiological cross-sectional area, and specialized sarcomere length operating range (Ward et al., 2009).

In terms of design, the range over which sarcomeres operate and their passive mechanical properties are also functionally relevant. For example, it has been demonstrated that wrist flexors and extensors operate on opposite sides of the sarcomere length–tension curve, and have similar elastic moduli, which causes a precise mechanical balance between flexion and extension moments throughout the range of wrist motion (Lieber and Fridén, 1998). It has also been demonstrated that passive material properties of muscles do not simply scale between the single-fiber and fiber-bundle levels (Lieber et al., 2003). In the multifidus, it has been demonstrated that the muscle operates almost exclusively on the ascending limb of its length–tension curve even though the passive mechanical properties of its cells are similar to other extremity muscles (Ward et al., 2009). However, without understanding the single-fiber and fiber-bundle passive mechanical behaviors of each key lumbar spine muscle it is impossible to determine whether such properties are characteristic of all lumbar extensors or unique to the multifidus.

Previous research showed that passive mechanical properties of single muscle fibers vary between muscles (Prado et al., 2005) and with disease state (Fridén and Lieber, 2003). In these studies, the changes in single-fiber intrinsic mechanical properties were likely due to reorganization of intracellular load–bearing proteins. Since it is the major source of intracellular passive tension, a change in titin isoform would be the most likely cause of passive fiber elasticity modulation at the cellular level (Prado et al., 2005). Importantly, it has been shown that changes in passive tension are not limited to single muscle cells. For example, in spastic muscle fiber bundles, it has been suggested that extracellular matrix has important to passive mechanical load-bearing properties (Lieber et al., 2003). However, the passive mechanical properties and titin isoforms are virtually unknown for the human lumbar spinal musculature.

Therefore purposes of this study were: (1) to compare single-fiber and fiber-bundle passive mechanical properties of the multifidus, longissimus, and iliocostalis muscles, (2) to measure the titin isoform size in each muscle, and (3) to determine the relationship between titin size and passive single-fiber and fiber-bundle mechanical properties in each muscle. Given what is currently known about the architecture of each muscle, the operating range of the multifidus, and the passive mechanical properties of muscle, we hypothesized that multifidus would have larger elastic modulus and smaller titin isoforms compared to longissimus or iliocostalis muscles.

2. Materials and methods

2.1. Specimen and preparation

Under a University of California San Diego Human Subjects Protection Program approved protocol, muscle specimens were obtained from patients undergoing spinal surgery (Table 1). Using minimally invasive retractors placed in the intermuscular planes between the multifidus and longissimus, and the longissimus and iliocostalis muscles it was possible to identify each of these muscles. A small segment of the muscle was isolated by blunt dissection along natural fascicular planes. A specialized clamp was then slipped over the bundle with care to avoid undue manipulation or tension on the muscle. After harvest, the biopsy was immediately placed in relaxing solution composed of (in millimoles per liter): ethylene–glycol tetraacetic acid (EGTA), 7.5; potassium propionate, 170; magnesium acetate, 2; imidazole, 5; creatine phosphate, 10; adenosine triphosphate (ATP), 4; leupeptin, a protease inhibitor, 17 mg/ml; and E64 (a protease inhibitor) 4 mg/ml (Wood et al., 1975). This solution prevented depolarization across any site of disrupted membrane and proteolytic degradation, either of which can destroy the specimen. Single fibers or fiber bundles were either immediately dissected from the fresh biopsy or placed into a storage solution composed of relaxing solution mixed with 50% glycerol and stored at −20 °C. Samples stored in this manner have been shown to have stable mechanical properties for up to 3 months (Wood et al., 1975; Moss, 1979), but all fibers in this study were tested within 14 days.

Table 1
Patient demographics.

Muscle	*n*-size	Age	Gender		Biopsy level			
			Male	Female	L2–L3	L3–L4	L4–L5	L5–S1
Multifidus	23	57 ± 14[a]	11	12	1	2	5	15
Longissimus	7	69 ± 10	3	4	–	3	4	–
Iliocostalis	7	69 ± 10	3	4	–	3	4	–

Values are mean ± SD.
[a] Significant difference between multifidus and longissimus–iliocostalis.

2.2. Passive single-fiber and fiber-bundle mechanics

The single- and fiber-bundle testing protocol was designed to measure elastic material properties apart from any velocity dependent properties, as previously described (Fung, 1981; Fridén and Lieber, 2003; Lieber et al., 2003). Briefly, the dissected fiber or fiber-bundle segment was secured on either side to 125 μm titanium wires using 10-0 silk suture loops. One wire was secured to an ultrasensitive force transducer (Model 405A, sensitivity 10 V/g, Aurora Scientific, Ontario, Canada) and the other was secured to a micromanipulator. The sample was transilluminated by a 7 mW He–Ne laser to permit sarcomere length measurement by laser diffraction (Lieber et al., 1984). Resolution of this method is approximately 5 nm (Baskin et al., 1979). The system was calibrated with a 2.50 μm plastic blazed diffraction grating prior to experimentation (Diffraction Gratings, Inc., Nashville, TN). After calibration and mounting, samples were lengthened until force registered on a load cell that defined baseline load and slack sarcomere length. Baseline sample diameters were optically measured with a cross-hair reticule mounted on a dissecting microscope and micromanipulators on an x–y mobile stage. Force–displacement data were generated for each mounted sample in 250 μm increments after which stress-relaxation was permitted for 2 min and both sarcomere length and tension were again recorded. Segments were elongated through the theoretical limit of actin and myosin overlap in human muscle (Lieber et al., 1994). Force data were converted to stress by dividing force by the baseline cross-sectional area value and displacement was converted to strain subtracting sarcomere length from the baseline slack sarcomere length value and then dividing by the baseline slack sarcomere length value. The slope of the stress–strain curve between 2.0 and 4.25 μm was defined as the elastic modulus. Samples were discarded if they did not produce a clear diffraction pattern, if any irregularities appeared along their length, or if they were severed or slipped at either suture attachment point during the test.

2.3. Analysis of titin isoform

Single fibers were homogenized in sodium dodecyl sulfate-vertical agarose gel electrophoresis (SDS-VAGE) sample buffer and stored at −80 °C until analyzed by gel electrophoresis. SDS-VAGE sample buffer was comprised of 8 M urea, 2 M thiourea, 3% SDS w/v, 75 mM DTT, 0.03% bromophenol blue, and 0.05 M Tris–Cl, pH 6.8 (Warren et al., 2003). The molecular mass of titin in single fibers was determined using SDS-VAGE. This procedure has been described previously (Warren et al., 2003). An acrylamide plug was placed at the bottom of the gel to hold the agarose in place. The final composition of this plug was 12.8% acrylamide, 10% v/v glycerol, 0.5 M Tris–Cl, 2.34% N,N′-diallyltartardiamide, 0.028% ammonium persulfate, and 0.152% TEMED. The composition of the agarose gel was 1% w/v Sea Kem Gold agarose (Lonza, Basel, Switzerland), 30% v/v glycerol, 50 mM Tris–base, 0.384 M glycine, and 0.1% w/v SDS. This solution was poured over the acrylamide plug and kept warm to prevent premature solidification.

Titin standards were obtained from human cadaver soleus and rat cardiac muscle, which have known molecular weights of 3700 and 2992 kDa, respectively, based on sequence analysis of the 300 kb titin gene with a coding sequence contained within 363 exons (Labeit and Kolmerer, 1995; Freiburg et al., 2000). These tissues were also homogenized and stored at −80 °C until analysis. Before loading onto the gel, a titin standards "cocktail" was created by placing 4 μL human soleus standard and 8 μL rat cardiac standard into 98 μL sample buffer. Sample wells were then loaded with both biopsy and rat cardiac homogenate. Human soleus and rat cardiac titin homogenates were loaded into standard lanes. This facilitated titin quantification on each gel. Gels were run at 4 °C for 5 h at 15 mA constant current.

Agarose gels were fixed and stained according to the Silver Stain Plus (Bio-Rad, Hercules, CA) procedure except that gels were dried for approximately 20 h at 40 °C

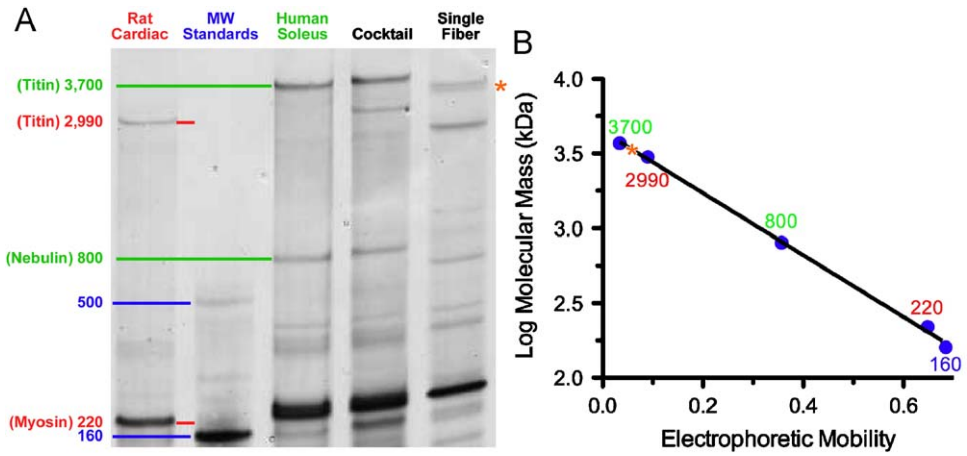

Fig. 1. Relative mobilities of proteins are linearly related to the log of their molecular mass. The gel regression relationship is calculated based on the three standard lanes containing rat cardiac titin, molecular weight standards, and human soleus titin (A). Relative mobilities of unknown titins are calculated based on the relative position of unknown (single fiber) bands compared to the standards. The molecular mass of the unknown band is then calculated from the relative mobility and the regression equation (B).

Table 2
Biomechanical testing of single fiber and fiber bundles.

Muscle	Single fiber				Fiber bundle		
	Diameter (mm)	Sarcomere length (μm)	*E* (kPa)	Titin MW (kD)	Diameter (mm)	Sarcomere length (μm)	*E* (kPa)
Multifidus	0.105±0.004	2.08±0.04	33.71±1.89	3581.7±13.9	0.317±0.02	2.06±0.03*	91.34±6.87*
Longissimus	0.095±0.005	2.25±0.04	32.80±3.22	3561.0±11.5	0.328±0.019	2.17±0.03	62.85±14.67
Iliocostalis	0.105±0.006	2.17±0.06	37.05±3.73	3562.4±6.2	0.332±0.019	2.19±0.04	58.83±7.74

Values are mean±SE.
* Significantly different ($p<0.05$) than longissimus and iliocostalis muscles.

immediately after fixing. Gels were subsequently rinsed and stained as described in the Silver Stain Plus procedure. Relative mobility and intensity of each band was quantified using a GS-800 Calibrated Densitometer (Bio-Rad) and Quantity One 1-D Analysis software (Bio-Rad).

Relative mobilities of proteins on the gel were linearly related to the log of their molecular mass (Fig. 1). The gel regression relationship was calculated based on the three standard lanes containing human soleus titin and rat cardiac titin. Relative mobilities of the biopsy samples were calculated based on their relative position compared to standards. The molecular mass of the unknown band was calculated from the relative mobility and the regression equation.

2.4. Data analysis

Three separate single-fiber and fiber-bundle passive mechanics experiments were averaged to obtain a single value per biopsy. Between muscle comparisons of fiber and bundle diameter, slack sarcomere length, elastic modulus, and titin molecular weight were made using one-way analyses of variance after screening data for normality and homogeneity of variances. When significant differences were identified for each dependent variable, *post-hoc* LSD tests were used to identify differences between individual muscles. As a control, linear regression was used to determine if there were significant relationships between age and dependent measurement. Simple linear regression also was used to determine the correlation between titin molecular mass and single-fiber and fiber-bundle elastic moduli. All values are reported as mean±standard error unless otherwise noted. Statistical tests were made using SPSS (version 16.0, Chicago, IL, USA) with *p*-values set to 0.05.

3. Results

Single-fiber diameters, slack sarcomere lengths, and elastic moduli were not significantly different among multifidus, longissimus, and iliocostalis muscles (Table 2 and Fig. 2A). Although fiber-bundle diameters were not different between muscles, slack sarcomere length was shorter ($p<0.05$) in the multifidus (2.06±0.03 μm) compared to longissimus (2.17±0.03 μm) and iliocostalis (2.19±0.04 μm) muscle bundles (Table 2. Similarly, fiber-bundle elastic modulus was 45% greater ($p<0.05$) in the multifidus (91.34±3.87 kPa) compared to longissimus (62.85±14.67 kPa) and iliocostalis (58.83±7.74 kPa) muscle bundles (Table 2 and Fig. 2B). Although patients in the multifidus muscle group were younger on average ($p<0.05$) than patients in the longissimus or iliocostalis groups (Table 1), there was no significant relationship between age and any mechanical parameter.

Titin molecular mass was nearly identical among single fibers of each muscle, ranging from 3561 to 3582 kD (Table 2). Given this narrow range of molecular masses, it was not surprising that titin molecular mass did not correlate with single-fiber or fiber-bundle slack sarcomere length or elastic modulus. Interestingly, when all muscles were considered, together, there was a significant but weak correlation ($r^2=0.117$, $p=0.038$) between single-fiber elastic modulus and fiber-bundle elastic modulus (Fig. 3) revealing only a weak scaling relationship between single-fiber and fiber-bundle passive mechanical properties. When muscles were considered individually, there was no correlation between multifidus or iliocostalis single-fiber and fiber-bundle elastic moduli, but in the longissimus muscle, this relationship was strong ($r^2=0.906$, $p=0.001$).

4. Discussion

The purposes of this study were: (1) to compare single-fiber and fiber-bundle passive mechanical properties of the multifidus, longissimus, and iliocostalis muscles, (2) to measure the titin isoform size in each muscle, and (3) to determine the relationship between titin size and passive single-fiber and fiber-bundle

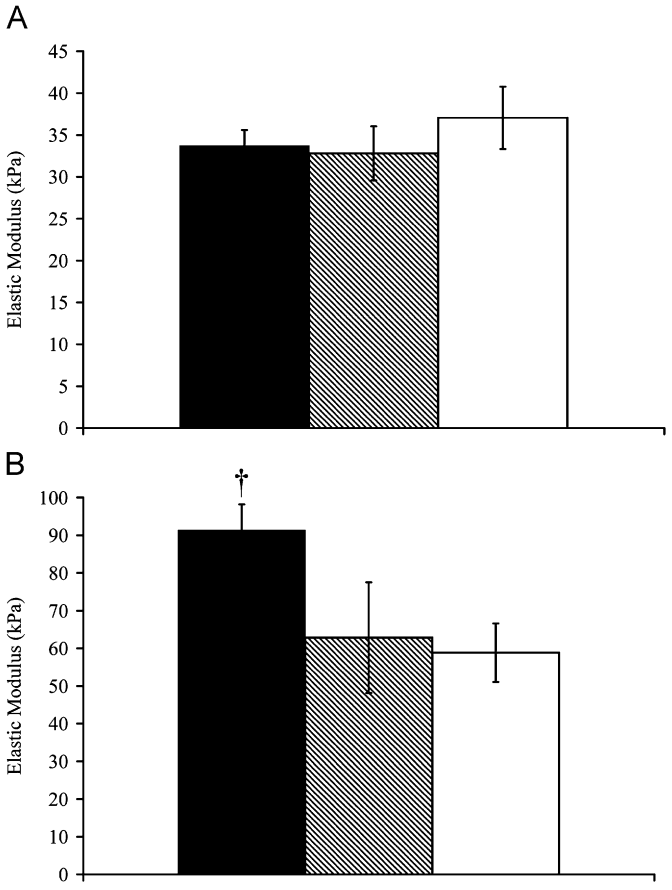

Fig. 2. Comparison of single fiber (A) and fiber bundle (B) elastic moduli in the multifidus (black bars), longissimus (hatched bars), and iliocostalis (white bars) muscles. Moduli were calculated as the slopes of the stress–strain curves in the range of 2.0–4.25 μm. † indicates significant differences between multifidus and longissimus and iliocostalis. Data are presented as mean ± SE.

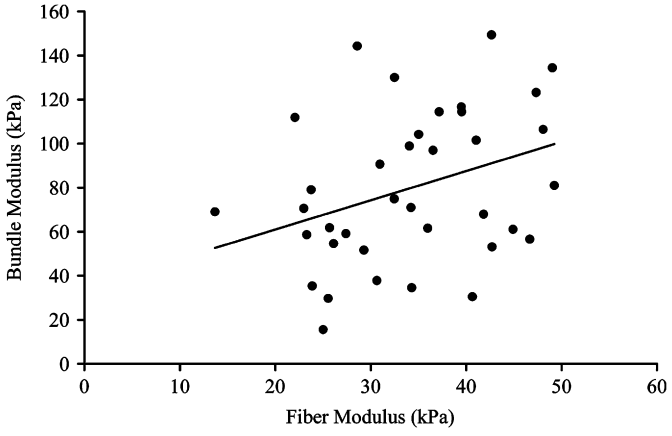

Fig. 3. Scatter plot of single-fiber elastic modulus (*x*-axis) versus fiber bundle elastic modulus (*y*-axis). For all muscles, single-fiber modulus only explained 12% of the variance in fiber bundle modulus; bundle modulus = 34.49+1.33(single-fiber modulus). This suggests that the passive mechanical properties of these muscles do not simply scale from the level of a single fiber to larger sizes.

mechanical properties in each muscle. We hypothesized that multifidus would have a higher elastic modulus and smaller titin isoform mass compared to longissimus or iliocostalis muscles. However, we found that, at the single-fiber level, all muscles had similar material properties. This finding agreed with the fact that titin isoform sizes were similar between muscles. It was not until muscles were observed at the fiber-bundle level, that differences were observed. Importantly, it appears that each muscle may have a different scaling relationship between the single-fiber and fiber-bundle level, suggesting that the structures responsible for higher order passive mechanical properties may be muscle specific.

There are several limitations to this study. First, our samples were obtained from individuals scheduled for a primary spine surgery indicating that some pathological process was already present at the time of the biopsy and thus, the muscle may not be truly "normal." Second, we arbitrarily limited the sarcomere length range over which elastic modulus was computed. This allowed us to limit our values to the theoretical limit of actin and myosin overlap in human muscle. However, ideally, we could estimate the modulus over the true physiologic range of sarcomere lengths experienced by each muscle. Unfortunately, these data are only available for multifidus muscle (Ward et al., 2009). Third, our elastic modulus measurements were limited to small samples (~9 fibers), with bundles approximately three times the diameter of single fibers. Ideally, for the purposes of scaling passive mechanical properties, we would test elastic modulus at multiple size scales including the whole muscle. Of course, this was impossible based on the limited size of the biopsies we were able to obtain. Fourth, our inability to identify significant correlations between titin molecular mass and slack sarcomere length or elastic modulus, may simply be due to the narrow range and similarity in titin molecular weights observed in these muscles.

At the single-fiber level, muscles had slack sarcomere lengths in the 2.08–2.25 μm range which is similar to. This range with the slack sarcomere length of the vastus lateralis (2.39 ± 0.28 μm) (Boakes et al., 2007) and a variety of antebrachial muscles (extensor digitorum, extensor pollicis, brachioradialis, etc.) (2.20 ± 0.04 μm) (Fridén and Lieber, 2003). Similarly, muscles had passive elastic moduli in the 32–38 kPa range which is similar to human vastus lateralis (32 ± 4.3 kPa) (Boakes et al., 2007) and a variety of human upper extremity muscles (28.25 ± 3.31 kPa) (Fridén and Lieber, 2003). Other studies have reported slightly smaller modulus values in control (16–21 kPa) and spinal cord injured patients (19–21 kPa) (Malisoux et al., 2007). However, this difference may be due to the smaller maximum sarcomere length achieved in this study. Thus, there does not appear to be a great deal of variability in passive material properties of human muscle fibers across muscles.

At the fiber-bundle level, the slack sarcomere lengths of the longissimus (2.17 μm) and iliocostalis (2.19 μm) muscles were similar but longer compared to the multifidus muscle (2.06 μm). The passive mechanical properties of the longissimus (62.8 kPa) and the iliocostalis (58.8 kPa) were also similar but nearly 50% smaller than multifidus (91.3 kPa). Given the similarity in single-fiber elastic moduli and titin isoform sizes, bundle slack sarcomere length and elastic moduli is determined by something other than titin size. Although speculative, it may be that these processes are determined by the properties of the extracellular matrix.

The fact that titin mass was not different among muscles was not surprising given the similarity among muscles in terms of single-fiber slack sarcomere length and elastic modulus, as it has been suggested that titin mass regulates these parameters (Wang et al., 1993; Prado et al., 2005). The fact that there was a weak correlation ($r^2 = 0.117$) between single-fiber and fiber-bundle passive mechanical properties across all muscles was interesting. This suggests that the scaling relationships between single fiber and fiber bundles are weak. However, when individual muscles were considered, there was in fact, no relationship between these variables in the multifidus and iliocostalis muscles, but a very strong relationship ($r^2 = 0.906$) in the longissimus. This finding

was significant despite the fact that the longissimus sample size was only 1/3 that of the multifidus, making it even more impressive.

An important consideration in spine surgery is the trauma caused to the posterior musculature during standard open posterior midline approaches, as injury has been shown to change muscle material properties (Gimbel et al., 2004). During open laminectomy procedures the spinous processes from which the multifidus muscle originates, are removed. Moreover, disruption of the multifidus neurovascular supply can be damaged by direct injury and by prolonged compression of the muscle by self-retaining retractor blades, leading to adverse histological and biochemical changes (Kawaguchi et al., 1994; Weber et al., 1997). Current minimally invasive surgical (MIS) procedures developed for spine surgery offer the unique opportunity to perform the same surgical procedures with less disruption to the spine musculature. These results provide the framework for testing the effects of disease, revision surgeries, and age on the passive mechanical properties of these important spinal muscles. *A priori* it could be argued that an alteration in the passive mechanical properties of each muscle, or an alteration in the relative passive mechanical properties between muscles, could adversely affect lumbar stability.

These data are the first direct quantification of passive single-fiber and fiber-bundle mechanical properties and titin isoforms of posterior lumbar musculature. Our results suggest that divergent passive material properties are observed at size scales larger than the single cell level, highlighting the importance of the extracellular matrix in these muscles. In addition to the architectural data previously reported (Ward et al., 2009), these data further support the unique stabilizing function of the multifidus muscle. These data will provide key input variables for biomechanical modeling of normal and pathologic lumbar spine function and direct future work in biomechanical testing in these important muscles.

Conflict of interest statement

The authors do not have conflicts of interest to disclose.

Acknowledgements

The authors wish to thank Dr. Marion Greaser for teaching us the SDS-VAGE technique used to measure titin molecular mass. This work was supported by the Department of Veterans Affairs Rehabilitation Research and Development, NIH grants HD048501 and HD050837.

References

Baskin, R.J., Roos, K.P., Yeh, Y., 1979. Light diffraction study of single skeletal muscle fibers. Biophys. J. 28, 45–64.

Boakes, J.L., Foran, J., Ward, S.R., Lieber, R.L., 2007. Muscle adaptation by serial sarcomere addition 1 year after femoral lengthening. Clin. Orthop. Relat. Res. 456, 250–253.

Bogduk, N., Macintosh, J.E., Pearcy, M.J., 1992. A universal model of the lumbar back muscles in the upright position. Spine 17 (8), 897–913.

Boswell, M.V., Trescot, A.M., Datta, S., Schultz, D.M., Hansen, H.C., Abdi, S., Sehgal, N., Shah, R.V., Singh, V., Benyamin, R.M., Patel, V.B., Buenaventura, R.M., Colson, J.D., Cordner, H.J., Epter, R.S., Jasper, J.F., Dunbar, E.E., Atluri, S.L., Bowman, R.C., Deer, T.R., Swicegood, J.R., Staats, P.S., Smith, H.S., Burton, A.W., Kloth, D.S., Giordano, J., Manchikanti, L., 2007. Interventional techniques: evidence-based practice guidelines in the management of chronic spinal pain. Pain Physician 10 (1), 7–111.

Chan, Y.L., Cheng, J.C., Guo, X., King, A.D., Griffith, J.F., Metreweli, C., 1999. MRI evaluation of multifidus muscles in adolescent idiopathic scoliosis. Pediatr. Radiol. 29 (5), 360–363.

Delp, S.L., Suryanarayanan, S., Murray, W.M., Uhlir, J., Triolo, R.J., 2001. Architecture of the rectus abdominis, quadratus lumborum and erector spinae. J. Biomech. 34 (3), 371–375.

Flicker, P.L., Fleckenstein, J.L., Ferry, K., Payne, J., Ward, C., Mayer, T., Parkey, R.W., Peshock, R.M., 1993. Lumbar muscle usage in chronic low back pain. Magnetic resonance image evaluation. Spine 18 (5), 582–586.

Freiburg, A., Trombitas, K., Hell, W., Cazorla, O., Fougerousse, F., Centner, T., Kolmerer, B., Witt, C., Beckmann, J.S., Gregorio, C.C., Granzier, H., Labeit, S., 2000. Series of exon-skipping events in the elastic spring region of titin as the structural basis for myofibrillar elastic diversity. Circ. Res. 86 (11), 1114–1121.

Fridén, J., Lieber, R.L., 2003. Spastic muscle cells are shorter and stiffer than normal cells. Muscle & Nerve 27, 157–164.

Friederich, J.A., Brand, R.A., 1990. Muscle fiber architecture in the human lower limb. J. Biomech. 23, 91–95.

Fung, Y.C., 1981. Biomechanics: Mechanical Properties of Living Tissues. Springer, New York.

Gille, O., Jolivet, E., Dousset, V., Degrise, C., Obeid, I., Vital, J.M., Skalli, W., 2007. Erector spinae muscle changes on magnetic resonance imaging following lumbar surgery through a posterior approach. Spine 32 (11), 1236–1241.

Gimbel, J.A., Van Kleunen, J.P., Mehta, S., Perry, S.M., Williams, G.R., Soslowsky, L.J., 2004. Supraspinatus tendon organizational and mechanical properties in a chronic rotator cuff tear animal model. J. Biomech. 37 (5), 739–749.

Hazard, R.G., 2006. Failed back surgery syndrome: surgical and nonsurgical approaches. Clin. Orthop. Relat. Res. 443, 228–232.

Jacobson, M.D., Raab, R., Fazeli, B.M., Abrams, R.A., Botte, M.J., Lieber, R.L., 1992. Architectural design of the human intrinsic hand muscles. J. Hand Surg. (Am. Vol.) 17A (804), 804–809.

Kang, C.H., Shin, M.J., Kim, S.M., Lee, S.H., Lee, C.S., 2007. MRI of paraspinal muscles in lumbar degenerative kyphosis patients and control patients with chronic low back pain. Clin. Radiol. 62 (5), 479–486.

Kawaguchi, Y., Matsui, H., Tsuji, H., 1994. Back muscle injury after posterior lumbar spine surgery. Part 1: histologic and histochemical analyses in rats. Spine 19 (22), 2590–2597.

Labeit, S., Kolmerer, B., 1995. Titins: giant proteins in charge of muscle ultrastructure and elasticity. Science (Washington, DC) 270, 293–296.

Lieber, R.L., Friden, J., 2001. Clinical significance of skeletal muscle architecture. Clin. Orthop. Relat. Res. 383 (383), 140–151.

Lieber, R.L., Fridén, J., 1998. Musculoskeletal balance of the human wrist elucidated using intraoperative laser diffraction. J. Electromyogr. Kinesiol. 8, 93–100.

Lieber, R.L., Jacobson, M.D., Fazeli, B.M., Abrams, R.A., Botte, M.J., 1992. Architecture of selected muscles of the arm and forearm: anatomy and implications for tendon transfer. J. Hand Surg. (Am. Vol.) 17A, 787–798.

Lieber, R.L., Loren, G.J., Fridén, J., 1994. In vivo measurement of human wrist extensor muscle sarcomere length changes. J. Neurophysiol. 71, 874–881.

Lieber, R.L., Runesson, E., Einarsson, F., Fridén, J., 2003. Inferior mechanical properties of spastic muscle bundles due to hypertrophic but compromised extracellular matrix material. Muscle & Nerve 28, 464–471.

Lieber, R.L., Yeh, Y., Baskin, R.J., 1984. Sarcomere length determination using laser diffraction. Effect of beam and fiber diameter. Biophys. J. 45, 1007–1016.

Macintosh, J.E., Bogduk, N., 1986. The biomechanics of the lumbar multifidus. Clin. Biomech. 1, 205–213.

Macintosh, J.E., Pearcy, M.J., Bogduk, N., 1993. The axial torque of the lumbar back muscles: torsion strength of the back muscles. Aust. N. Z. J. Surg. 63 (3), 205–212.

Malisoux, L., Jamart, C., Delplace, K., Nielens, H., Francaux, M., Theisen, D., 2007. Effect of long-term muscle paralysis on human single fiber mechanics. J. Appl. Physiol. 102 (1), 340–349.

Moss, R.L., 1979. Sarcomere length-tension relations of frog skinned muscle fibers during calcium activation at short lengths. J. Physiol. (London) 292, 177–192.

Parkkola, R., Rytokoski, U., Kormano, M., 1993. Magnetic resonance imaging of the discs and trunk muscles in patients with chronic low back pain and healthy control subjects. Spine 18 (7), 830–836.

Powell, P.L., Roy, R.R., Kanim, P., Bello, M., Edgerton, V.R., 1984. Predictability of skeletal muscle tension from architectural determinations in guinea pig hindlimbs. J. Appl. Physiol. 57, 1715–1721.

Prado, L.G., Makarenko, I., Andresen, C., Kruger, M., Opitz, C.A., Linke, W.A., 2005. Isoform diversity of giant proteins in relation to passive and active contractile properties of rabbit skeletal muscles. J. Gen. Physiol. 126 (5), 461–480.

Rantanen, J., Rissanen, A., Kalimo, H., 1994. Lumbar muscle fiber size and type distribution in normal subjects. Eur. Spine. J. 3 (6), 331–335.

Rosatelli, A.L., Ravichandiran, K., Agur, A.M., 2008. Three-dimensional study of the musculotendinous architecture of lumbar multifidus and its functional implications. Clin. Anat.

Sasaoka, R., Nakamura, H., Konishi, S., Nagayama, R., Suzuki, E., Terai, H., Takaoka, K., 2006. Objective assessment of reduced invasiveness in MED. Compared with conventional one-level laminotomy. Eur. Spine J. 15 (5), 577–582.

Sihvonen, T., Herno, A., Paljarvi, L., Airaksinen, O., Partanen, J., Tapaninaho, A., 1993. Local denervation atrophy of paraspinal muscles in postoperative failed back syndrome. Spine 18 (5), 575–581.

Skaf, G., Bouclaous, C., Alaraj, A., Chamoun, R., 2005. Clinical outcome of surgical treatment of failed back surgery syndrome. Surg. Neurol. 64 (6), 483–488 (Discussion 488–9).

Stokes, I.A., Gardner-Morse, M., 1999. Quantitative anatomy of the lumbar musculature. J. Biomech. 32 (3), 311–316.

Taylor, R.S., 2006. Spinal cord stimulation in complex regional pain syndrome and refractory neuropathic back and leg pain/failed back surgery syndrome: results

of a systematic review and meta-analysis. J. Pain Symptom Manage 31 (4 Suppl), S13–S19.
Turner, J.A., Loeser, J.D., Deyo, R.A., Sanders, S.B., 2004. Spinal cord stimulation for patients with failed back surgery syndrome or complex regional pain syndrome: a systematic review of effectiveness and complications. Pain 108 (1–2), 137–147.
Wang, K., McCarter, R., Wright, J., Beverly, J., Ramirez-Mitchell, R., 1993. Viscoelasticity of the sarcomere matrix of skeletal muscles. The titin–myosin composite filament is a dual-stage molecular spring. Biophys. J. 64, 1161–1177.
Ward, S.R., Kim, C.W., Eng, C.M., Gottschalk, G.L., Tomiya, A., Garfin, S.R., Lieber, R.L., 2009. Architectural analysis and intraoperative measurements demonstrate the unique design of the multifidus muscle for lumbar spine stability. J. Bone Joint Surg. 91 (1), 176–185.
Warren, C.M., Krzesinski, P.R., Greaser, M.L., 2003. Vertical agarose gel electrophoresis and electroblotting of high-molecular-weight proteins. Electrophoresis 24, 1695–1702.
Weber, B.R., Grob, D., Dvorak, J., Muntener, M., 1997. Posterior surgical approach to the lumbar spine and its effect on the multifidus muscle. Spine 22 (15), 1765–1772.
Wickiewicz, T.L., Roy, R.R., Powell, P.L., Edgerton, V.R., 1983. Muscle architecture of the human lower limb. Clin. Orthop. Rel. Res. 179, 275–283.
Wood, D.J., Zollman, J., Reuban, J.P., Brandt, P.W., 1975. Human skeletal muscle: properties of the "chemically skinned" fiber. Science (Washington, DC) 187, 1075–1076.
Zhao, W.P., Kawaguchi, Y., Matsui, H., Kanamori, M., Kimura, T., 2000. Histochemistry and morphology of the multifidus muscle in lumbar disc herniation: comparative study between diseased and normal sides. Spine 25 (17), 2191–2199.